OUTDOOR AIR TEMPERATURE EFFECTS ON HEAT RECOVERY VENTILATOR PERFORMANCE

A Thesis

by

TROY PANGAN AÑORA

Submitted to the Office of Graduate and Professional Studies of
Texas A&M University
in partial fulfillment of the requirements for the degree of

MASTER OF SCIENCE

Chair of Committee,	Michael B. Pate
Committee Members,	Harry A. Hogan
	Pavel V. Tsvetkov
Head of Department,	Andreas A. Polycarpou

December 2020

Major Subject: Mechanical Engineering

ABSTRACT

Heat recovery ventilators, or HRVs, exhaust stale indoor air and supply fresh outdoor air while also transferring heat between the two airstreams via a heat exchange core. Considering the energy efficiency and energy savings of HRVs, a thesis project was inspired that focused on the thermal performance of these devices. In particular, this thesis project centered on: (1) designing, developing, and constructing a test setup for data collection on recovery ventilators based on Canadian Standards Association standard C439, (2) using the test setup to generate a data base of HRV test data for a wide range of outdoor air temperatures, and (3) investigating the effects of outdoor air temperature on the apparent effectiveness and sensible heat-recovery efficiency of an HRV with the intention of promoting applications and improving operations.

A major goal of this research is to investigate HRV performance as characterized by two important parameters, namely, the apparent effectiveness, ε, and sensible heat-recovery efficiency, E_{SHR}. In support of this investigation, a total of 33 tests were conducted on the Fantech SHR200 HRV unit, and then this data file was used to determine the unit's ε and E_{SHR} for a range of representative hot outdoor air temperatures, namely, 88 °F to 112 °F, while maintaining a rated volumetric flowrate of approximately 195 CFM. During testing, these supply inlet airstream temperatures were achieved via an electric duct heater, which in turn enabled the HRV to perform in the cooling mode.

The results from the 33 tests showed proportional relationships for both ε and E_{SHR} parameters versus outdoor air temperature. Apparent effectiveness, ε, increased slightly from 55% to 60% as the hot outdoor air temperature increased from about 88 °F to 112 °F. A plot of ε versus outdoor air temperature fit with a linear regression produced an R-squared value of 0.3155, indicating that the linear model partially fits the data. The sensible heat-recovery efficiency E_{SHR}

increased from 32% to 48% as the hot outdoor air temperature increased over the aforementioned min-to-max range, namely, about 88 °F to 112 °F. For E_{SHR} versus outdoor air temperature, the R-squared value of the linear regression was 0.7540, indicating that most of the linear model fits the data. In comparison, the parameter E_{SHR} versus outdoor air temperature is better fitted by a linear model compared to the parameter ε versus outdoor air temperature. Even so, the application of a linear trendline for both data sets was verified through a p-test and by plotting residuals versus fits and normal probability plots. Such verification was necessary to substantiate the statistical significance of both parameters, ε and E_{SHR}, with outdoor air temperature.

Based on an analysis of the HRV, engineers can be assured that the apparent effectiveness, ε, and sensible heat-recovery efficiency, E_{SHR}, of an HRV does not suffer or worsen as the hot outdoor air temperature increases, which is an important and even somewhat unexpected finding. On the contrary, the observed 5% increase in ε (55% to 60%) and the observed 16% increase in E_{SHR} (32% to 48%) suggests that HRV performance adapts and even improves as hot outdoor air temperature rises. These performance results support adopting HRVs for use in improving indoor air quality while increasing one's confidence that HRVs can lead to energy efficiency and savings even in hot outdoor air temperatures.

DEDICATION

I would like to dedicate this thesis to my mom, Araceli, and my dad, Michael, for their love, support, and selfless sacrifices made throughout my life and academic career; to my sister, Mikka, for being a mentor and guiding force in my life; to my grandparents for their love and allowing me to access better opportunities in life; to the Pangan and Añora families for their constant support; and finally to my friends and support systems who have encouraged me throughout my undergraduate and graduate studies.

I am humbled and eternally grateful for these people for always believing in me and the efforts I put towards my pursuits in life. To God be the glory forever and ever. Thank you.

ACKNOWLEDGMENTS

I would like to thank my committee chair, Dr. Pate, for his guidance with this thesis project and for offering me the opportunity to work at REEL while funding my studies. I would also like to thank Dr. Hogan and Dr. Tsvetkov for their willingness to serve as my committee members.

I would like to thank my friends and coworkers at REEL for their support with my research endeavors.

CONTRIBUTORS AND FUNDING SOURCES

Contributors

This work was supervised by a thesis committee comprised of Professor PATE (advisor) and HOGAN of the Department of Mechanical Engineering and Professor TSVETKOV of the Department of Nuclear Engineering.

Funding Sources

Graduate study was supported by an assistantship from Dr. PATE and the Energy Systems Laboratory.

NOMENCLATURE

CSA	Canadian Standards Association
HRV	Heat Recovery Ventilator
ε	Apparent Effectiveness
E_{SHR}	Sensible Heat-Recovery Efficiency
ERV	Energy Recovery Ventilator

TABLE OF CONTENTS

Page

LIST OF FIGURES

Page

LIST OF TABLES

Page

1. INTRODUCTION

1.1 Background

Residential ventilation is a modern necessity because home living entails the production of unwanted moisture and harmful pollutants as a result of regular activities such as washing, showers, cooking, and appliance use. In essence, the lack of ventilation within a residential space creates an environment filled with stale air that decreases indoor air quality and overall comfort level for occupants. One solution for improving indoor air quality is to implement balanced, regular ventilation by using a heat recovery ventilator, or HRV. This device achieves regular ventilation while transferring heat between air supplied to and air exhausted from a ventilated space thus promoting energy efficiency and energy savings. In summary, heat recovery ventilators aid in maintaining residential comfort levels by supplying fresh air and cooling an airstream as needed. In this thesis project, a test setup was established for measuring HRV thermal performance in a laboratory setting, thus providing an increased understanding of HRV application and operations.

1.2 HRV Description and Operation

A heat recovery ventilator, or HRV, is a box unit that transfers heat between supply and exhaust airstreams that flow through the device. A standard HRV possesses two fans and a heat exchange core. The two fans serve the purpose of exhausting the indoor air from a space and supplying fresh outdoor air towards a space. The heat exchange core is the defining feature of a heat recovery ventilator [1]. The core transfers heat from the warmer airstream to the cooler airstream. For example, on a day with warm outdoor air such as during the summertime, the heat would be transferred from the supply air, which comes from the hot outdoors, to the exhaust

airstream in order to cool the incoming air. The preceding example is defined as “cooling mode”, and this mode, applied to hot climates, is the focus of this study. Conversely, on a day with cold outdoor air such as during the wintertime, the heat would be transferred from the exhaust airstream to the supply airstream to warm the incoming air. The preceding example is defined as “heating mode”, which has been the historical focus of HRVs, especially because of large energy consumption for heating buildings in cold climates. The supply and exhaust airstreams travel through multiple narrow passages inside the heat exchange core and alternate, and it is important to note that there is no mixing of the airstreams. As mentioned above, the focus of the facility described herein and the data gathered and evaluated focuses on the HRV cooling mode.

Heat recovery ventilators vary in performance levels. Some HRVs are rated for up to 85% heat recovery, and a standard HRV for residential use is rated for moving about 200 CFM of air. Some HRVs also possess adjustable fan speeds to meet the air quality needs for individual residences. In addition, in regards to indoor air quality, HRVs have installed filters that act as barriers for unwanted contaminants including dust and pollen. Overall, HRVs are suitable for homes that are well-sealed in order to continuously replace stale air with dry, fresh air. In this project, the focus will be on the cooling mode operation of a heat recovery ventilator as affected by incoming air temperature from the outdoor environment.

1.3 Objective

The objective of this project is to use data measurements taken on an HRV to evaluate heat recovery ventilator performance in the cooling mode, which is the dominant mode for hot climates, by using two parameters, namely, the apparent effectiveness ε and sensible heat-recovery efficiency E_{SHR}. This performance study will center on varying the outdoor air temperature that

enters the recovery ventilation system and then evaluating the effects on the apparent effectiveness and sensible heat-recovery efficiency with the goal of providing guidance for HRV applications and operations.

1.4 Scope

The scope of this research that is required to achieve the previously mentioned objectives includes these major tasks: (1) designing, developing, and constructing a well-instrumented facility to test actual HRVs under realistic conditions, (2) acquiring a large test data set for a typical HRV operating with hot outdoor air temperature in cooling mode, and (3) determining the apparent effectiveness and sensible heat-recovery efficiency of an HRV for a wide range of hot-air test conditions. Part of the test rig establishment included constructing a mounting system for recovery ventilators of various shapes, sizes, technologies, and mounting methods. Next, the test rig was set up with a wide range of instruments for acquiring data including air velocity, volumetric flow rate, temperature, relative humidity, and static pressure. As part of the rig design process, a number of the requirements outlined in Canadian Standards Association (CSA) standard C439 for testing heat recovery ventilators were incorporated in the new facility [2].

After completing the instrument facility and setup, extensive testing was performed on a typical HRV and the requisite data was gathered for a wide range of test conditions, including, temperature and flow rates. For these test conditions and the resulting data set, apparent effectivenesses and sensible heat-recovery efficiencies were determined with the intention of improving HRV application and operations.

2. TEST SETUP

The experimental setup for studying the performance of heat recovery ventilators involves the ventilator at the center of a test rig with metal ducts connected to the ventilator ports. The HRV used in this study is the Fantech SHR200. The metal ducts are 6 inches in diameter, approximately 103 inches in length, and each duct has a 90° elbow to prevent mixing of air prior to entering the duct system. Each HRV is installed according to the manufacturer's recommended method in order to simulate realistic operation conditions. For example, one method of HRV installation is by suspending an HRV on a pair of chains from support beams. The suspension installation method was followed for the Fantech SHR200 unit. Various sensors (which are discussed in the following section) are lined along each duct to measure relevant performance data such as temperature, static pressure, and air velocity. All of the sensors are wired to data acquisition cards in order to record and send data to a local computer. A schematic diagram of the test setup with an HRV installed is presented in the following Figure 1.

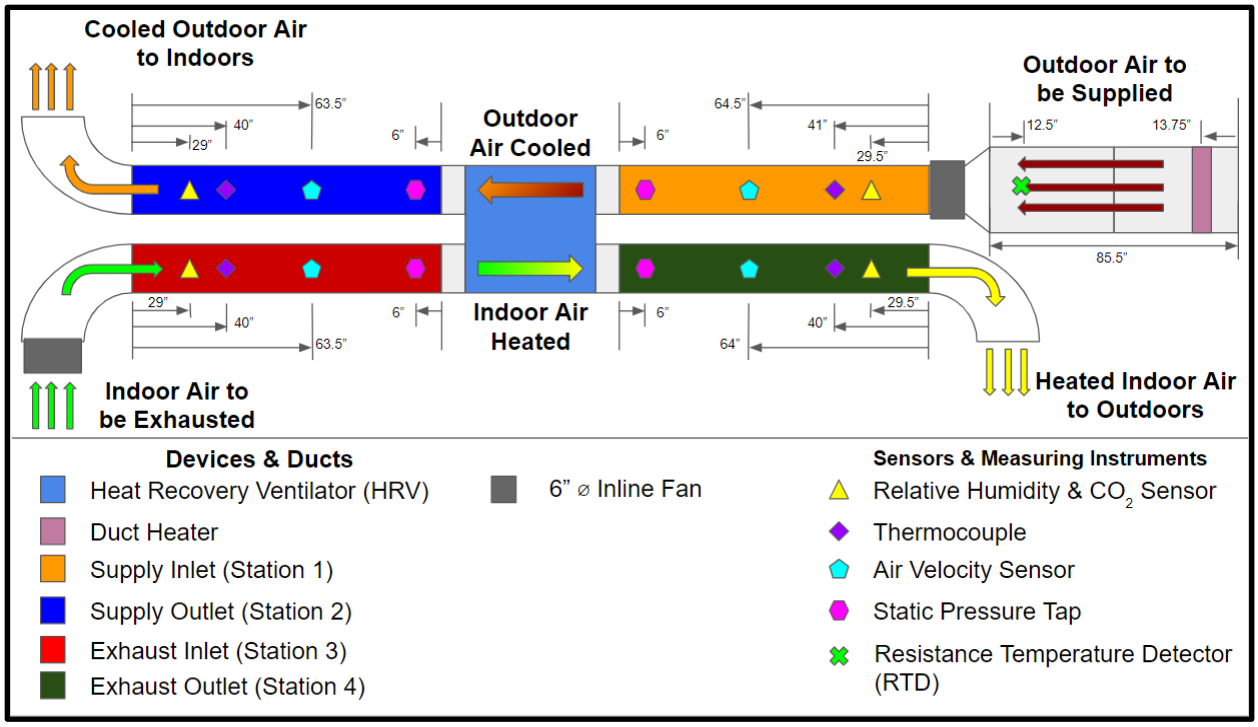

Figure 1. A schematic diagram of the HRV test setup

The preceding Figure 1 provides a top-down view of the test setup. Figure 1 features colors that identify the distinct stations, such as supply inlet, that will be referenced throughout this thesis. Figure 1 also features the sensor locations as well as their relative distance to the ends of the ducts. Lastly, Figure 1 includes arrows that depict the flow of air for the supply airstream as well as the exhaust airstream. The airstream colors indicate either heating or cooling that is taking effect as the airstream passes through the HRV. For the outdoor air that is to be supplied indoors, the airstream changes color from red to orange as the airstream is losing heat when passing through the HRV. For the indoor air that is to be exhausted to the outdoors, the airstream changes color from green to yellow as the airstream is gaining heat when passing through the HRV. Within the HRV, the colors gradients for the arrows in the supply and exhaust airstreams reflect the change in heat as air moves through the heat exchange core. The HRV and its two internal fans drive the

airstreams while the inline fans at the supply inlet and exhaust inlet assist with balancing the airflow throughout the duct system.

The supply inlet duct that connects to the HRV is connected to an immersion heater that raises the temperature of incoming air. The immersion heater assists with varying the temperature of the supply inlet air to simulate hot outdoor air. Recalling the objective of the project, the outdoor air temperature will be varied and the impact on HRV performance will be observed. The following Figure 2 depicts the placement of the immersion heater in the rectangular duct that connects to supply inlet duct.

Figure 2. Front view of the immersion heater

As seen in the preceding Figure 2, the immersion heater is suspended from the top of a rectangular duct with an opening that is 12 inches wide and 23.5 inches tall. The immersion heater is a standard tubular duct heater manufactured by Tempco. The immersion heater is wired to a proportional-integral-derivative (PID) controller in order to have the heater temperature regulated. The PID controller will receive a set point temperature inputted by a user. The heater will attempt to achieve the set point temperature with the assistance of the PID controller. Said PID controller is also wired to a resistance temperature detector, or RTD, that is down the line from the immersion

heater. The RTD provides the feedback necessary for the PID to understand whether the temperature of the heater needs to be raised or lowered to achieve the user's inputted set point temperature.

The following Figure 3 illustrates the section of the test setup that houses the immersion heater and also provides a view of the exhaust outlet duct.

Figure 3. Section of test setup connected to immersion heater

In the preceding Figure 3, the rectangular duct is 85.5 inches in length and rests on a custom-fabricated steel support system. The rectangular duct then interfaces with an inline fan. The inline fan then connects to the supply inlet duct.

The ducts on the side of the HRV opposite to the side with the immersion heater are nearly identical to what was shown in Figure 3. This section of the test setup has one inlet duct and one outlet duct, each with a 90° elbow. Note that the inline fan that is normally connected to the exhaust inlet (duct facing the camera) was removed for clarity of the duct for the photo. The following Figure 4 illustrates the section of the test setup on the other side of the HRV installation area.

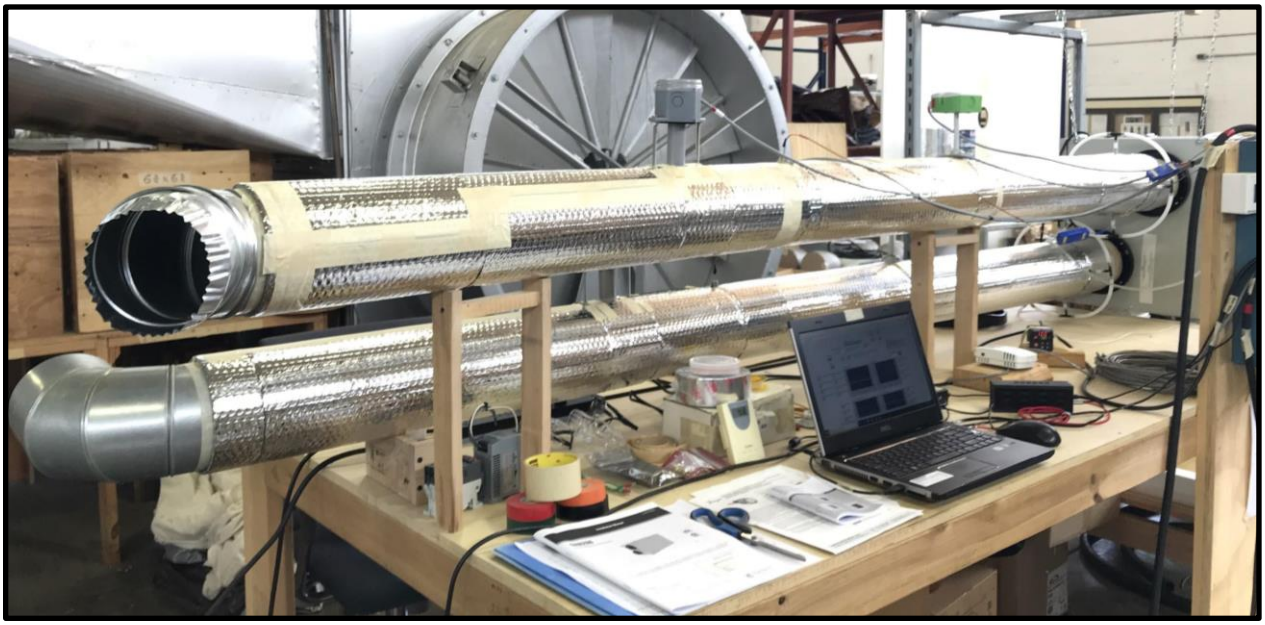

Figure 4. Section of test setup opposite of immersion heater side

To support an experimental goal of balanced ventilation within the test setup, two 6” diameter inline fans were added to the duct system. One inline fan was added to the supply inlet duct and the other inline fan was added to the exhaust inlet duct. The following Figure 5 depicts the inline fan that was installed at the supply inlet, namely, the Ostberg CK 6C.

Figure 5. Inline fan installed at supply inlet

The following Figure 6 depicts the inline fan that was installed at the exhaust inlet, namely, the Fantech Rn4EC-3.

Figure 6. Inline fan installed at exhaust inlet

The two inline fans added to the duct system helped achieve balanced airflow within the supply and exhaust airstreams. Balanced airflow is one of the requirements for a test to be conducted on an HRV, according to standard C439. The next section will discuss in detail the sensors that are installed along the ducts as seen in the previous figures.

3. INSTRUMENTATION AND SOFTWARE

To determine the apparent effectiveness and heat-recovery efficiency of a heat recovery ventilator, parameters such as temperature, static pressure, and air velocity must be observed and recorded during HRV operation. As such, various sensors that are designed to measure each parameter have been implemented into the test rig. The four main sensors that have been implemented are: CO_2 / relative humidity sensor, thermocouple, air velocity transmitter, and pressure transducer.

The CO_2 / relative humidity sensor is the Dwyer CDTR-2D4D4 and is depicted in the following Figure 7.

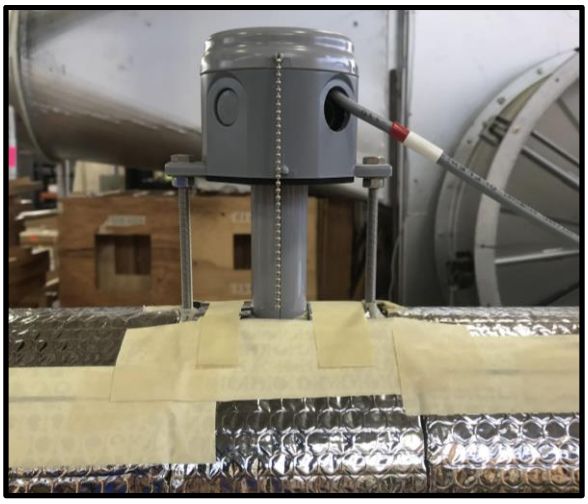

Figure 7. CO_2 and relative humidity sensor installed in duct

The Dwyer CDTR-2D4D4 is designed specifically for duct applications and as such is fitting for the HRV test setup. Each duct in the test setup houses a CO_2 / relative humidity sensor that is capable of measuring the carbon dioxide content and relative humidity of the air flowing through the duct. Although CO_2 content and relative humidity are not within the scope of this project, these parameters were still considered when establishing the test setup. As such, a sensor

capable of measuring both CO_2 and relative humidity was included in each duct as a means of preparing for future project scopes.

The thermocouple used in the test setup is the OMEGA Type T thermocouple and is featured in the following Figure 8.

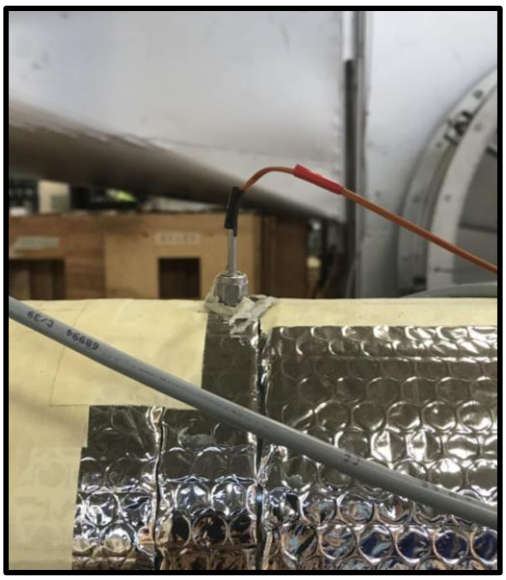

Figure 8. Type T thermocouple installed in duct

Each duct in the test setup houses a thermocouple to measure the temperature of the air flowing through the duct.

The air velocity transmitter used in the test setup is the E+E Elektronik EE650 air velocity transmitter and is depicted in the following Figure 9.

Figure 9. Air velocity transmitter installed in duct

The EE650 is designed specifically for HVAC applications and as such is fitting for the HRV performance study. Each duct in the test setup houses an air velocity transmitter that measures the velocity of the air flowing through the duct. The air velocity that is recorded is then used to compute the volumetric flow rate of the air. The computation is performed in a custom data recording software that was written by the author of this thesis in National Instruments' LabVIEW. A screenshot of the custom data recording software can be seen in the following Figure 10.

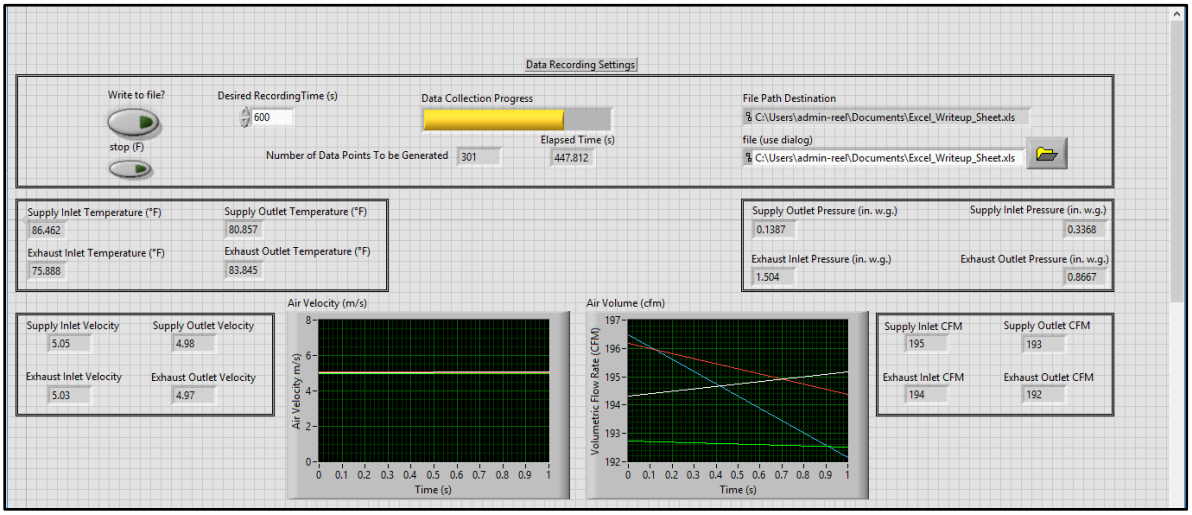

Figure 10. Screenshot of custom LabVIEW data recording software

The preceding Figure 10 reflects how the user is able to able to begin collecting data from the test setup via a graphical user interface. After data collection is complete using the recording software, the data is then exported to a Microsoft Excel file. The Microsoft Excel file containing the data is then processed within a custom-made spreadsheet by the author of this thesis. Said custom-made spreadsheet produces plots depicting information such as duct temperature over time from when the test was performed. Furthermore, the custom-made spreadsheet is also what computes the two HRV performance parameters, namely, apparent effectiveness and sensible heat-recovery efficiency.

The pressure transducer used in the test setup is the Setra Model 264 and is showcased in the following Figure 11.

Figure 11. Pressure transducer connected to the test setup duct

Each duct in the test setup houses a piezometer ring that has four connection points with the duct to measure static pressure. The piezometer ring is displayed in the following Figure 12 and was constructed in accordance with a pressure measurement standard [3].

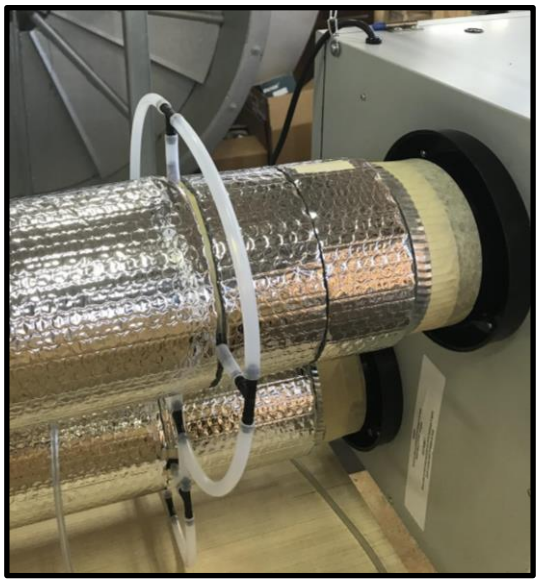

Figure 12. Piezometer ring attached to the test setup duct

The piezometer ring is connected to the Setra Model 264 pressure transducer to transmit static pressure readings to the data recording software.

Each sensor and instrument discussed in this section has an operating range and level of accuracy. These operating ranges and accuracy levels are fitting for studying heat recovery ventilators as required by CSA standard C439. In the Appendix of this thesis is the inclusion of Table 3, a table of operating ranges and measurement accuracies of the test setup sensors. The following section will discuss how the sensors are implemented into a methodology to acquire data on HRVs and characterize thermal operation.

4. METHODOLOGY

The test methodology was developed with the guidance of CSA testing standard C439, "Standard laboratory methods of test for rating the performance of heat/energy-recovery ventilators". The interest of this particular project is in the characterization of the performance of heat recovery ventilators as affected by outdoor air temperature. The following section will provide an overview of two key metrics that help characterize HRV performance.

4.1 HRV Performance Metrics

Two key metrics help characterize HRV performance, namely, apparent effectiveness and sensible heat-recovery efficiency.

Apparent effectiveness is calculated as shown by the following Equation 1:

$$\varepsilon = \frac{M_s \times (X_1 - X_2)}{M_{min} \times (X_1 - X_3)} \quad \text{(Eq. 1)}$$

where ε represents apparent sensible heat effectiveness, M_s represents the mass flow rate of the supply air (kg dry air / unit of time), X represents dry bulb temperature at the indicated duct location, and M_{min} represents M_s or M_e, whichever is less (with M_e representing the mass flow rate of the exhaust air). As a reminder, the duct locations can be referenced in Figure 1 of this thesis. Mass flow rate was calculated by multiplying the mean volumetric flow rate from a test by the air density. Dry bulb temperatures were averaged from the temperature sensor readings.

Sensible heat-recovery efficiency is calculated as shown by the following Equation 2:

$$E_{SHR} = \frac{\left(\sum_{i=1}^{n} M_{s,i} \times C_P \times \left(t_{2,i} - t_{1,i}\right) \times \triangle\theta\right) - Q_{SF}}{\left(\sum_{i=1}^{n} M_{max,i} \times C_P \times \left(t_{3,i} - t_{1,i}\right) \times \triangle\theta\right) + Q_{EF}} \quad \text{(Eq. 2)}$$

The following list defines each of the variables present in Equation 2:

E_{SHR} = sensible heat recovery efficiency

n = total number of measurements

i = *i*th tame that data are recorded

M_s = net mass flow rate of the supply air, kg/s

C_P = specific heat of air, kJ / (kg · K)

t_2 = net outdoor airflow temperature at station 2, ˚C

t_1, t_3 = dry-bulb temperature at stations 1 and 3, respectively, ˚C

$\triangle\theta$ = time between flow measurements, s

Q_{SF} = energy input into supply airstream attributed to fan(s), kJ

M_{max} = M_S or M_e , whichever is greater

Where

M_e = net mass flow rate of the exhaust air, kg/s

Q_{EF} = energy input into exhaust airstream attributed to fan(s), kJ

Each of the two preceding performance metrics are computed based on parameters involving temperature, static pressure, and air velocity. As such, the previously described sensors aid in capturing the parameters that feed into computing apparent effectiveness and sensible heat-recovery efficiency. In addition, it is important to note that the energy input attributed to fans along each exhaust stream was computed. The computation was made possible by recording data on the current and voltage draw of the inline fans using a clamp ammeter and multimeter, respectively.

With the test setup, instrumentation, data recording software, and key performance parameters now described, the necessary conditions to be met prior to testing will be discussed in the next subsection.

4.2 Conditions to Satisfy Prior to Data Collection

The following pre-test conditions were informed by CSA standard C439. Prior to collecting the pertinent data on a heat recovery ventilator, the test setup and sensors are inspected to ensure proper positioning and working condition. The measuring devices and the heat recovery ventilator are operated for no less than 1 hour prior to data collection. It is important to note that the HRV is to be tested with an electrical source at 60 Hz and 120 V AC unless otherwise specified by the manufacturer. In addition, the airflow across the HRV is to be balanced as per the HRV manufacturer's standards. In the case of the HRV for this project, the Fantech SHR200, an average volumetric flowrate of 195 CFM across the HRV is desired. After 1 hour has passed with the HRV being powered on, data is to be collected in 10-minute intervals. Pertinent values are measured by the sensors installed along the test rig and sent to a custom-made LabVIEW Virtual Instrument (VI) that keeps a running log of the collected data. For each set of data that is collected, a manual log entry is filled out by the operator of the test rig that includes information such as duct heater temperature, lab floor temperature, and data collection start time. The collected data is saved, exported, and analyzed to determine the apparent effectiveness and sensible heat-recovery efficiency of the HRV under study.

With the preceding outlined conditions satisfied, data was collected for a series of tests on the HRVs. The following section will present the data that was collected for the scope of this project. In addition, the following sections discuss the results and any implications that outdoor air temperature may have on HRV performance.

5. PRESENTATION OF DATA & DISCUSSION OF RESULTS

As previously mentioned, temperature data and volumetric flowrate data were collected from the test setup while varying a simulated outdoor air temperature. To simulate the outdoor air temperature, a standard tubular duct heater was connected to a proportional-integral-derivative (PID) controller. Said PID controller was also wired to a resistance temperature detector, or RTD, in order to monitor the changing outdoor air temperature. Through a combination of monitoring the outdoor temperature and regulating the power passed from a voltage source to the heater, the PID controller would maintain a set point temperature for the duct heater. Said set point temperature was treated as a simulation of the outdoor air temperature that would be associated with hot, fresh, outdoor air entering a building and passing through an HRV. In total, six outdoor air temperatures were simulated using six temperature set points for the duct heater, namely, 90 °F, 95 °F, 100 °F, 105 °F, 110 °F, and 115 °F. The apparent effectiveness and sensible heat-recovery efficiency that was computed at each of the temperature set points is presented through plots in the following sections.

5.1 Apparent Effectiveness

The following Figure 13 shows the average apparent effectiveness, ε, for each heater set point.

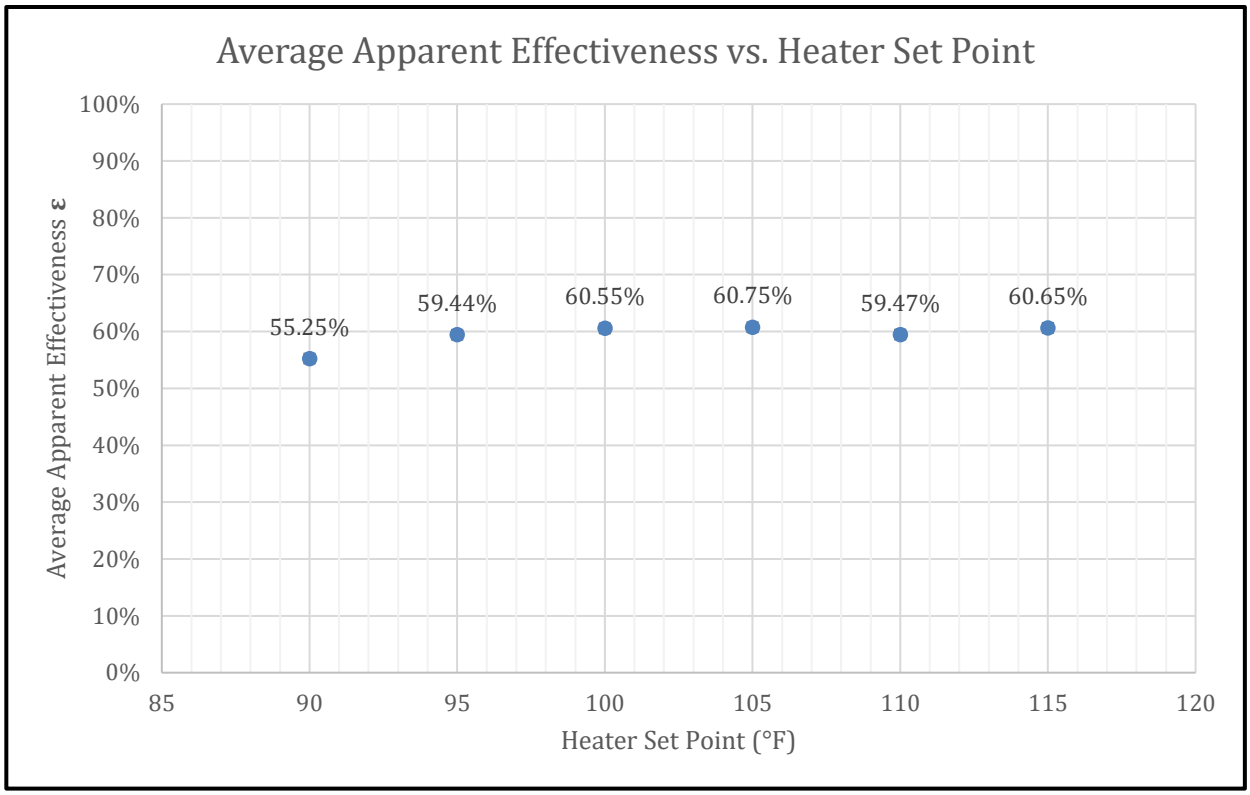

Figure 13. Average Apparent Effectiveness vs. Heater Set Point

At first glance, it can be observed from Figure 13 that there is little change in average ε as the heater set point temperature increases. One observation is that there is a slight increase in average ε as the heater set point increases from 90 °F to 95 °F. Beyond 95 °F, however, the average ε appears to settle. Each data point in Figure 13 represents the average ε at a heater set point temperature from five or six tests, depending on the heater set point. In addition, each data point in Figure 13 is labeled with the average ε value above the data marker along with vertical error bars that reflect the standard deviation from the average ε, or better known as standard error. The vertical error bars are difficult to see as they are mostly less than 1% in value. The standard error for each average ε at each heater set point is summarized in the following Table 1. Standard deviation was also included for each data set of average ε at each heater set point as standard deviation was needed to compute standard error.

Table 1. Standard Deviation and Standard Error for Average Apparent Effectiveness

Heater Set Pt. (°F)	Avg. ε	Std. Dev. Of Avg. ε	Std. Error Of Avg. ε
90	55.25%	2.60%	1.16%
95	59.44%	2.51%	1.03%
100	60.55%	1.98%	0.81%
105	60.75%	1.57%	0.70%
110	59.47%	1.83%	0.75%
115	60.65%	1.56%	0.70%

As shown in Table 1, the standard error of the average ε across the six heater set points is below 1.5%, with the maximum standard error being 1.16% at a heater set point of 90 °F and the minimum standard error being 0.70% at a heater set point of 105 °F and 115 °F.

The objective of this study is to determine the presence and nature of the effects that the outdoor air temperature has on heat recovery ventilator performance. With this objective in mind, a linear trendline was applied to Figure 13 in an attempt to best describe the relationship between average effectiveness ε and heater set point at this time.

The following Figure 14 showcases the application of the linear trendline, its corresponding equation, and its corresponding R-squared value, known as the coefficient of determination [4].

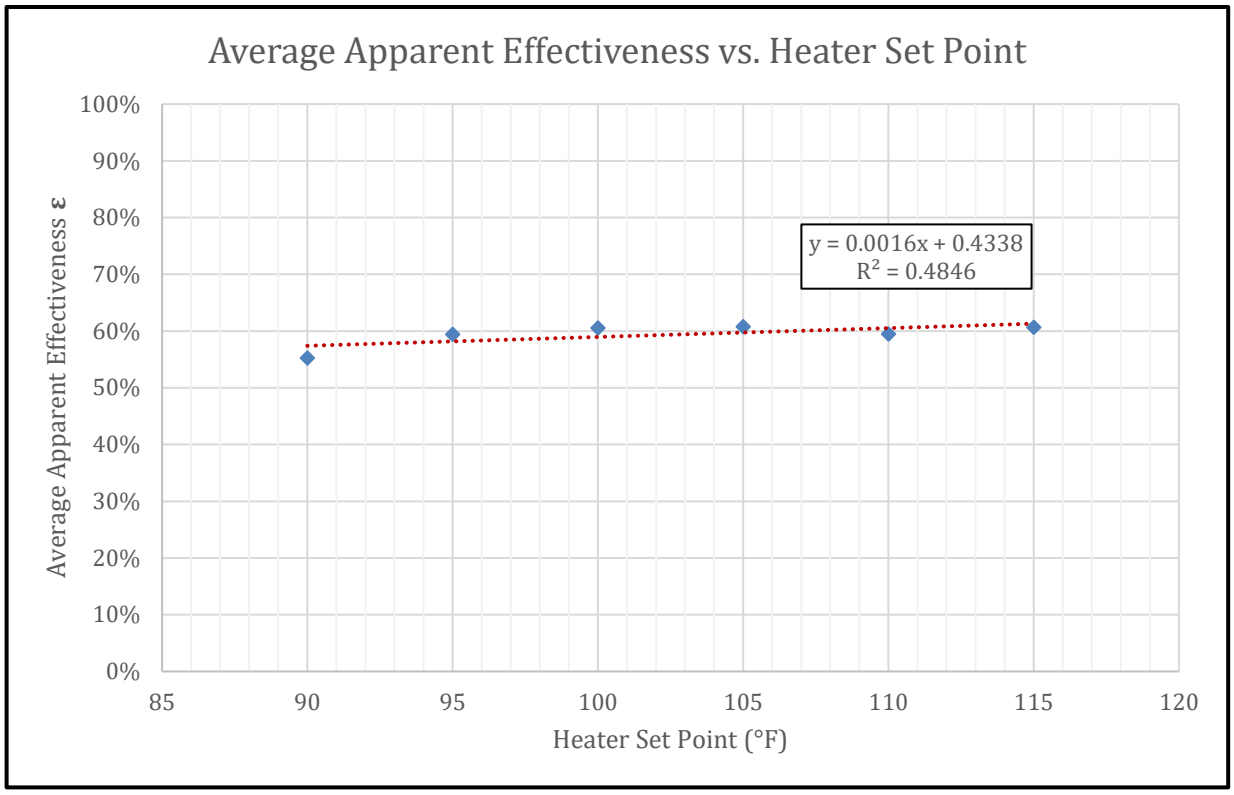

Figure 14. Linear Trendline Applied to Average ε vs. Heater Set Point

As shown in Figure 14, the coefficient representing the slope of the linear trendline is 0.0016 and the constant representing the intercept is 0.4338. Although low in magnitude, the positive nature of the coefficient in the trendline equation indicates a positive correlation between the average apparent effectiveness ε and heater set point. The R-squared value of the linear regression is 0.4846. R-squared is defined as the percentage of the response variable variation that is explained by the linear model [4]. In the case of the preceding plot, an R-squared value of 0.4846 conveys the notion that the linear model explains some of the variability of the response data (i.e. average apparent effectiveness) around its mean.

The preceding plots showcased the average ε that was computed from five or six tests at each heater set point. For a closer look and expanded view, the individual ε that was computed for each of the individual tests was also plotted against the average outdoor air temperature that was

measured during the test. As mentioned previously, the heater set point is a temperature that is selected on a PID controller. The PID controller, which is connected to the duct heater, is then tasked with regulating the heater set point temperature. Due to the variability of controllers, however, the duct heater will not maintain the heater set point at an exact temperature at all times. For example, setting the duct heater at a set point of 90 °F could result in the heater being heated up to 88 °F or 91 °F at a given time as the controller attempts to maintain the set point temperature. Thus, the supply inlet air temperature was monitored throughout the duration of each test and averaged to obtain an outdoor air temperature. The temperatures in the following plots reflect the average supply inlet air temperature from each test over a duration of 10 minutes.

The following Figure 15 is a plot that illustrates the apparent effectiveness ε that was computed for each test conducted for the study. In total, there are 33 data points, each reflecting a test that involved collection of temperature and volumetric flowrate data at an outdoor air temperature.

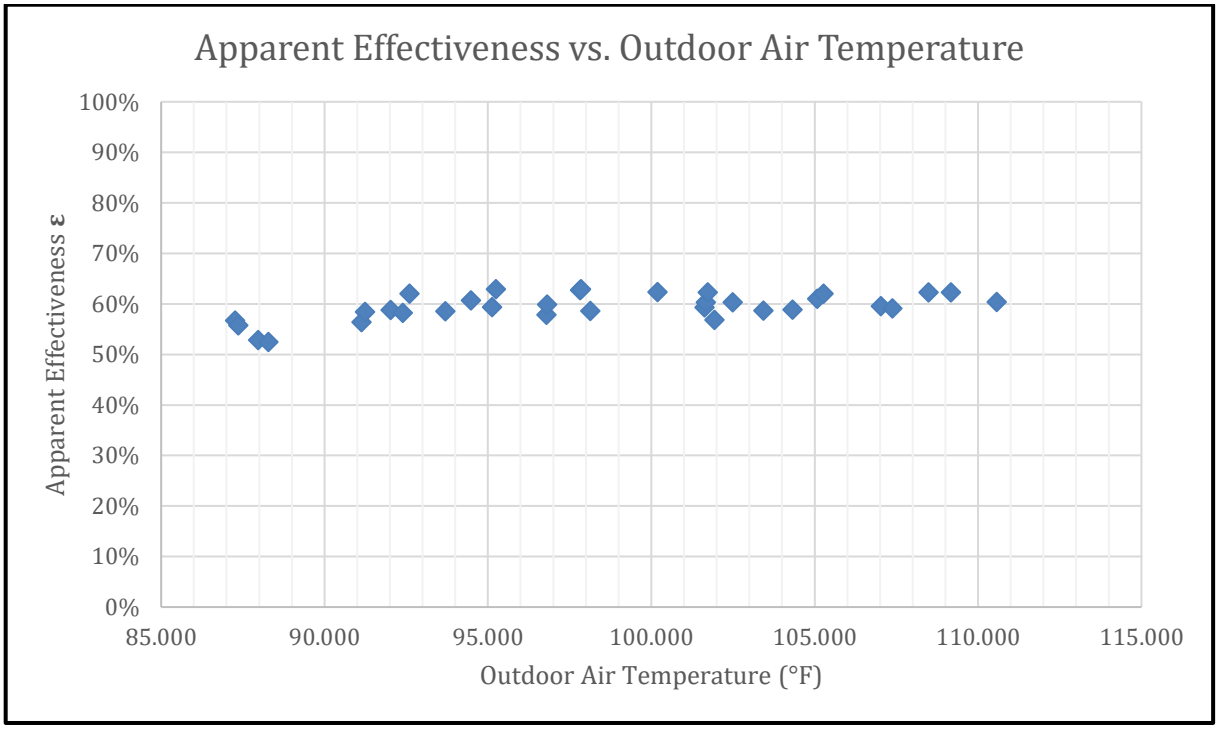

Figure 15. Apparent Effectiveness vs. Outdoor Air Temperature

From this data set, an observation can be made that the ε "plateaus" once the outdoor air temperature increases from approximately 87.5 °F to approximately 92.5 °F. To clarify, the "plateau" observation translates to ε neither increasing nor decreasing as the outdoor air temperature increases. Prior to the plateau, there is only a slightly increase in apparent effectiveness as the outdoor air temperature increases from approximately 87.5 °F to approximately 92.5 °F.

Similar to the treatment of the plot of average ε versus heater set point, a linear trendline was also applied to the plot of individual ε versus outdoor air temperature. Such treatment was applied in order to increase understanding and awareness of any relationships between outdoor air temperature and HRV performance.

The following Figure 16 showcases the application of the linear trendline, its corresponding equation, and its corresponding R-squared value.

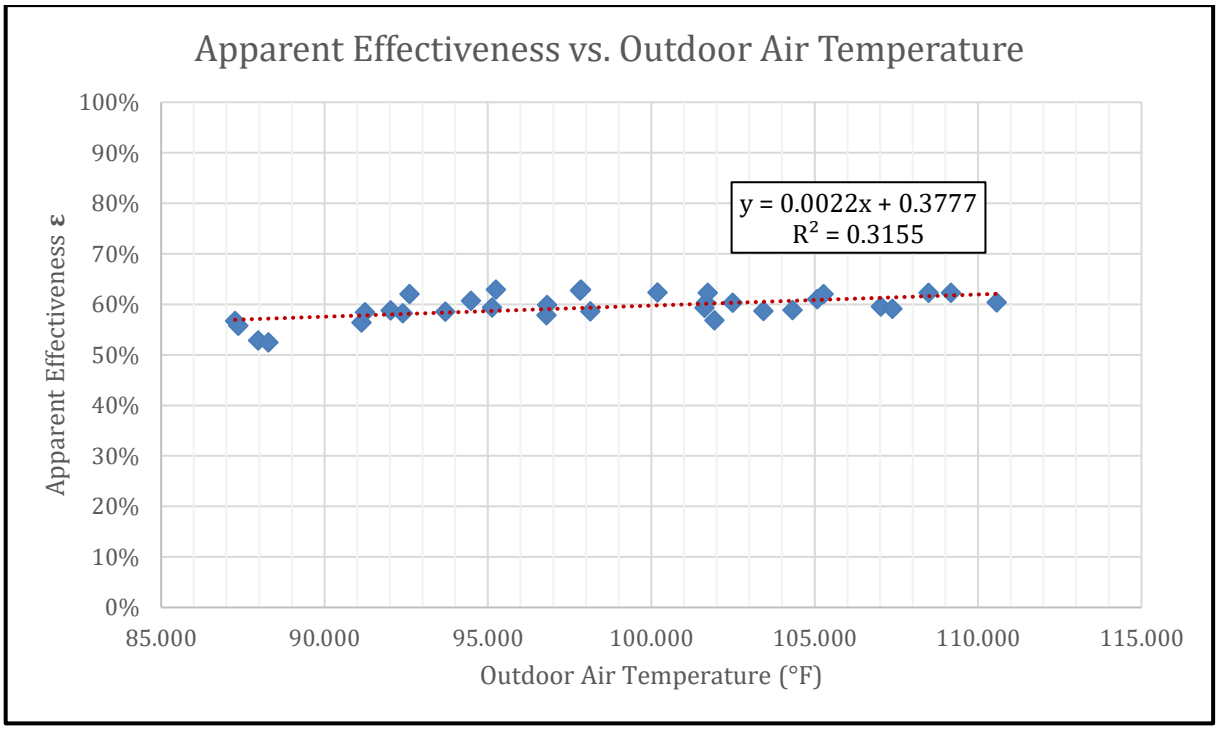

Figure 16. Linear Trendline Applied to ε vs. Outdoor Air Temperature

As shown in Figure 16, the coefficient representing the slope of the linear trendline is 0.0022 and the constant representing the intercept is 0.3777. Although low in magnitude, the positive nature of the coefficient in the trendline equation indicates a positive correlation between the apparent effectiveness ε and outdoor air temperature. The R-squared value is 0.3155, which indicates that the linear model explains some of the variability of the response data (i.e. apparent effectiveness) around its mean. Compared to the R-squared value from Figure 14, which was 0.4846, the R-squared value of 0.3155 for the linear trendline applied in Figure 16 is lower. Such a comparison was to be expected, however, as Figure 16 has increased data scatter as compared to Figure 14. Said data scatter is a result of taking an expanded view of the apparent effectiveness data. In Figure 14, the apparent effectiveness was averaged for all of the tests conducted at each heater set point. In Figure 16, the apparent effectiveness of each individual test is plotted against the recorded outdoor air temperature of each individual test. As such, the R-squared value of the linear trendline applied to the individual test data points is lower compared to the averaged test data points.

To continue the investigation, a determination of the statistical significance of the association between the response variable (apparent effectiveness) and the term (outdoor air temperature) was made. Such a determination was made by comparing the p-value of the term (outdoor air temperature) to a significance level of 0.05 to assess the null hypothesis [5]. In the case of this study, the null hypothesis is that the association between apparent effectiveness and outdoor air temperature is not statistically significant. Should the p-value of the linear regression be less than or equal to 0.05 (the significance level α), then the null hypothesis is rejected. After applying the linear regression shown in Figure 16 and utilizing the Data Analysis package in Microsoft Excel, it was found that the p-value for the term (outdoor air temperature) is

approximately 0.00067. Hence, with p-value < α, we reject the notion that the association is not statistically significant. Therefore, there is a statistically significant association between apparent effectiveness ε and outdoor air temperature.

In order to substantiate the linear regression model applied, two additional assumptions were verified. The first assumption that was verified was that the residuals are randomly distributed [5]. In statistics, residuals are defined as the difference between actual response variable value versus the fitted value offered by the linear model. A random distribution of residuals is examined via a plot of residuals versus fits. Ideally, there should be no recognizable pattern in the points within the plot of residuals versus fits. The following Figure 17 illustrates the residuals versus fits plot for the apparent effectiveness linear regression model.

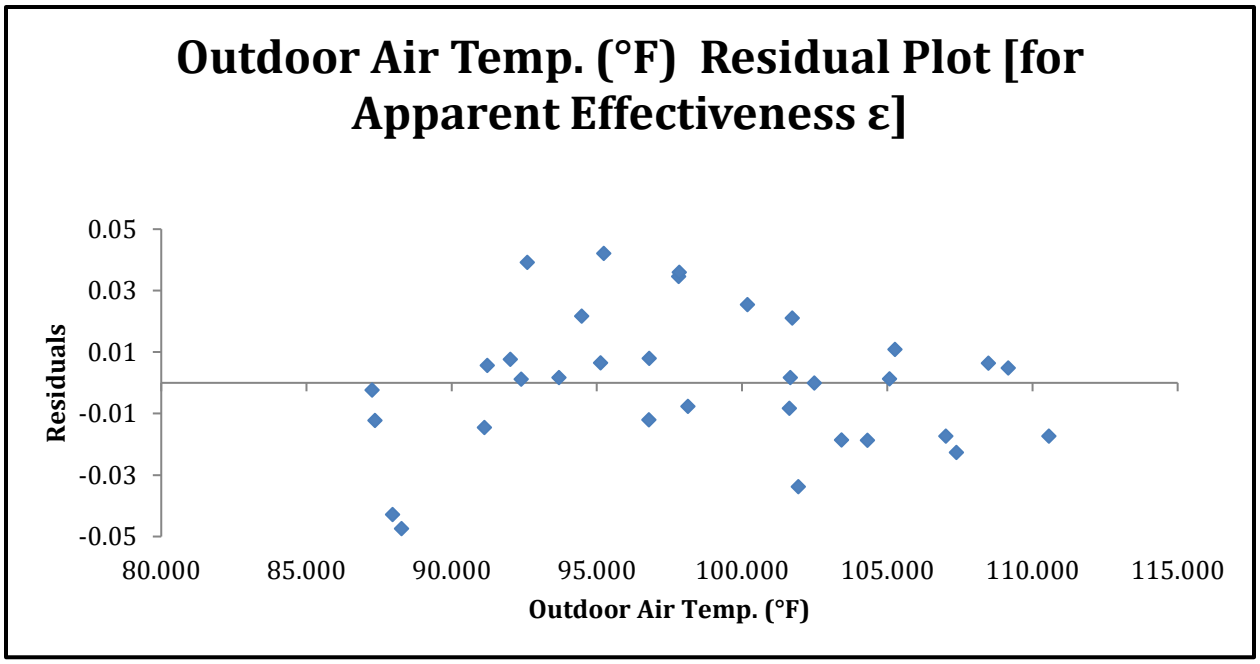

Figure 17. Residuals vs. fits plot for Apparent Effectiveness

As depicted in Figure 17, the points appear randomly scattered on the plot, which is ideal. It is worth noting that there are two outliers towards the bottom of the plot. The two outliers have residual values of approximately -0.05, indicating that the apparent effectiveness from these two

data points are lower than the fitted value offered by the linear regression. Despite the presence of these two outliers, the overall residuals versus fits plot has no identifiable pattern that is visible. Therefore, given the current data set, the first assumption of random distribution of residuals is verified. Conducting additional tests on the HRV for apparent effectiveness within the studied outdoor air temperature range is advisable for a strengthened verification.

There was previous mention of two assumptions to be verified in order to substantiate the linear regression model. The second assumption that was verified was that the residuals are normally distributed [5]. A normal distribution of residuals is examined via a normal probability plot. Ideally, the normal probability plot of the residuals should approximately follow a straight line. The following Figure 18 illustrates the normal probability plot for the apparent effectiveness linear regression model.

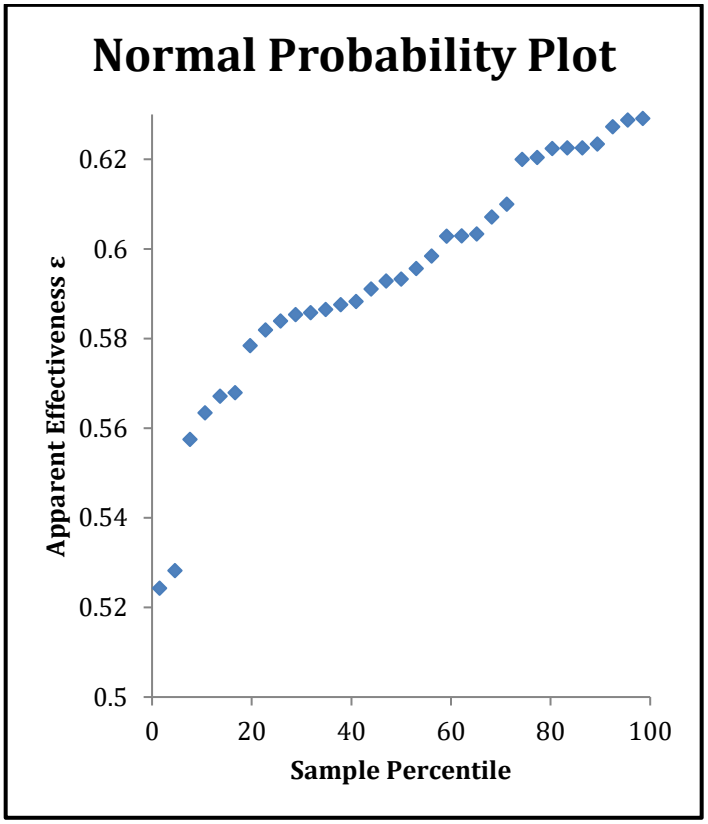

Figure 18. Normal probability plot for Apparent Effectiveness

As seen in Figure 18, a majority of the residuals generally appear to follow a straight line. However, there are two outliers, namely, the two residuals with apparent effectiveness values closer to 0.52, or 52%. The two outliers are the same as those identified in the plot of residuals versus fits in Figure 17. Assuming that the two outliers were potentially the result of inconsistent regulation of the duct heater temperature, then a reexamination of the normal probability plot can be made. The following Figure 19 illustrates the normal probability plot that was featured in Figure 18 minus the two outlier residuals.

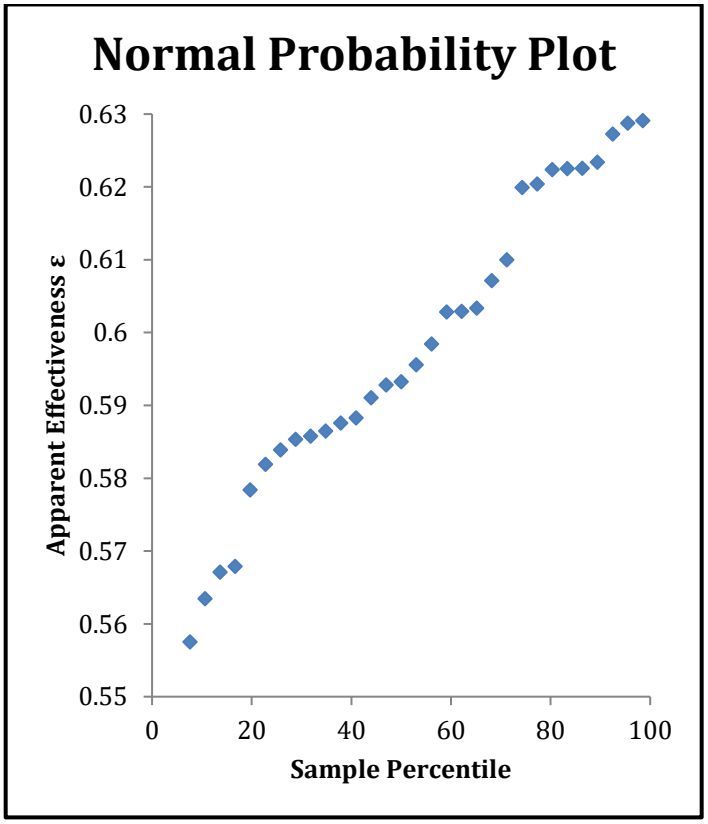

Figure 19. Outliers removed from ε normal probability plot

As depicted in Figure 19, the normal probability plot features residuals that appear to follow a straight line. With the outliers aside, it is assumed that the residuals are normally distributed in regards to the linear regression for apparent effectiveness. Said outliers could be the

result of inconsistencies during the data collection period of 10 minutes during testing. The inconsistencies could be sourced to uneven regulation of power to the duct heater or some deviations in performance for the fans in the duct system. A set of 33 data points meets the recommended minimum sample size of 30 for statistical analysis [6]. Should the two outliers be set aside as irregularities, the sample size would be reduced to 31 points. Ideally for future analysis, more tests would be conducted to produce a larger dataset.

The following section will discuss the data that was collected on sensible heat-recovery efficiency, another important parameter for characterizing HRV performance.

5.2 Sensible Heat-Recovery Efficiency

The following Figure 20 shows the average sensible heat-recovery efficiency, E_{SHR}, for each heater set point.

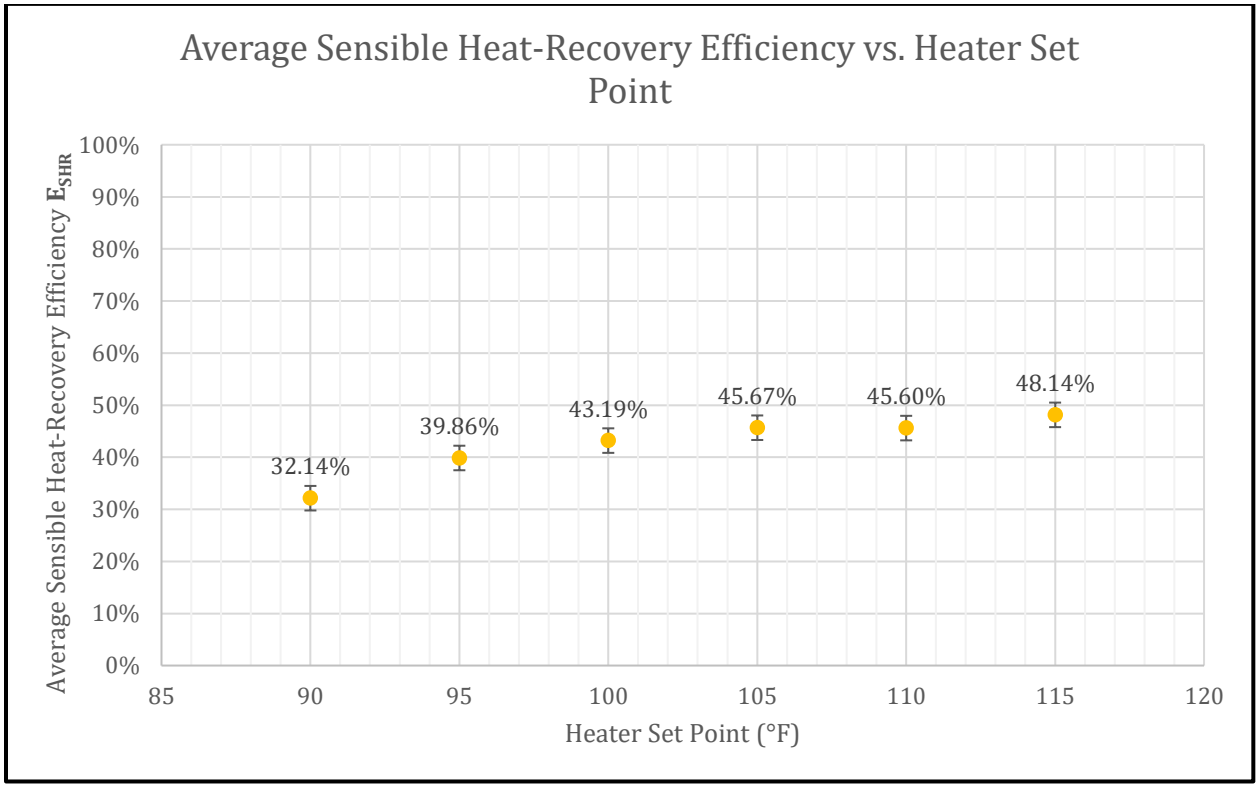

Figure 20. Average Sensible Heat-Recovery Efficiency vs. Heater Set Point

At first glance, it can be observed from Figure 20 that there is a positive trend between the average E_{SHR} and the heater set point temperature. As the heater set point temperature increases, the average E_{SHR} increases. Each data point in Figure 20 represents the average E_{SHR} at a heater set point temperature from five or six tests, depending on the heater set point. In addition, each data point in Figure 20 is labeled with the average E_{SHR} value above the data point along with vertical error bars that reflect the standard deviation from the average E_{SHR}, or better known as standard error. The standard error for each average E_{SHR} at each heater set point is summarized in the following Table 2. Standard deviation was also included for each data set of E_{SHR} at each heater set point as standard deviation was needed to compute standard error.

Table 2. Standard Deviation and Standard Error for Average Apparent E_{SHR}

Heater Set Pt. (°F)	Avg. E_{SHR}	Std. Dev of Avg. E_{SHR}	Std. Error of Avg. E_{SHR}
90	32.14%	4.94%	2.21%
95	39.86%	3.73%	1.52%
100	43.19%	2.50%	1.02%
105	45.67%	2.34%	1.05%
110	45.60%	2.59%	1.06%
115	48.14%	2.23%	1.00%

As shown in Table 2, the standard error of the average E_{SHR} across the six heater set points is below 2.5%, with the maximum standard error being 2.21% at a heater set point of 90 °F and the minimum standard error being 1.00% at a heater set point of 115 °F.

The objective of this study is to determine the presence and nature of the effects that the outdoor air temperature has on heat recovery ventilator performance. With this objective in mind, a linear trendline was applied to Figure 20 in an attempt to best describe the relationship between E_{SHR} and outdoor air temperature at this time.

The following Figure 21 showcases the application of the linear trendline, its corresponding equation, and its corresponding R-squared value.

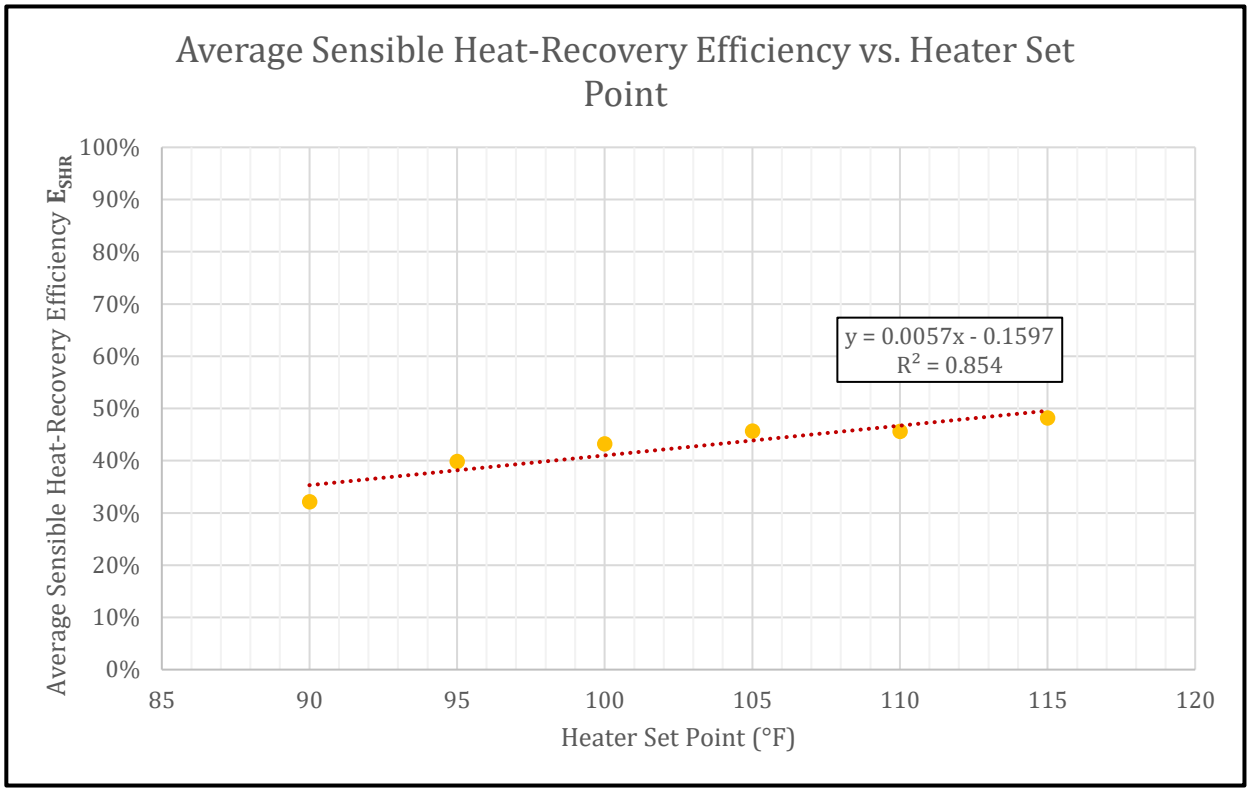

Figure 21. Linear Trendline Applied to Average E_{SHR} vs. Heater Set Point

As shown in Figure 21, the coefficient representing the slope of the linear trendline is 0.0057 and the constant representing the intercept is -0.1597. The R-squared value is 0.854. Although low in magnitude, the positive nature of the coefficient in the trendline equation indicates a positive correlation between the sensible heat-recovery efficiency E_{SHR} and outdoor air temperature. The R-squared value is 0.854, which conveys the notion that the linear model explains most of the variability of the response data (i.e. E_{SHR}) around its mean.

The preceding plots showcased the average E_{SHR} that was computed from five or six tests at each heater set point. For a closer look and akin to the approach of the apparent effectiveness ε data, the individual E_{SHR} that was computed for each of the individual tests was also plotted against

the average outdoor air temperature that was measured during the test. The temperatures in the following plots reflect the average supply inlet air temperature from each test over a duration of 10 minutes.

The following Figure 22 is a plot that illustrates the E_{SHR} that was computed for each test conducted for the study. In total, there are 33 data points, each reflecting a test that involved collection on temperature and volumetric flowrate data at an outdoor air temperature.

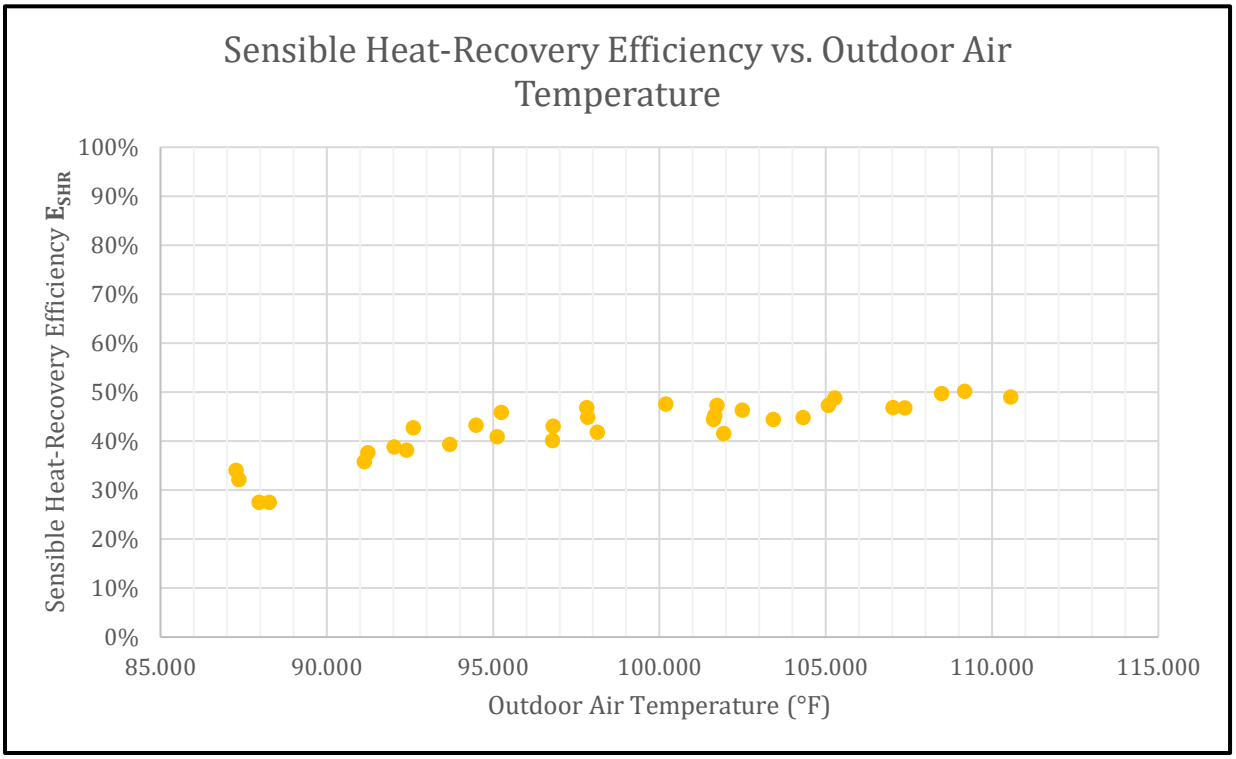

Figure 22. Sensible Heat-Recovery Efficiency vs. Outdoor Air Temperature

At first glance, it can be observed from Figure 22 that there is a slight positive trend between the E_{SHR} and the outdoor air temperature. As the outdoor air temperature increases, the E_{SHR} increases. From this data set, a second observation can be made that the E_{SHR} "plateaus" as the outdoor air temperature increases beyond 100 °F. To clarify, the "plateau" observation translates to the E_{SHR} not increasing as much as the outdoor air temperature increases beyond 100

°F as compared to when the outdoor air temperature increases between approximately the 87.5 °F to 97.5 °F range.

Similar to the treatment of the plot of average E_{SHR} versus heater set point, a linear trendline was also applied to the plot of individual E_{SHR} versus outdoor air temperature. Such treatment was applied in order to increase understanding and awareness of any relationships between outdoor air temperature and HRV performance.

The following Figure 23 showcases the application of the linear trendline, its corresponding equation, and its corresponding R-squared value.

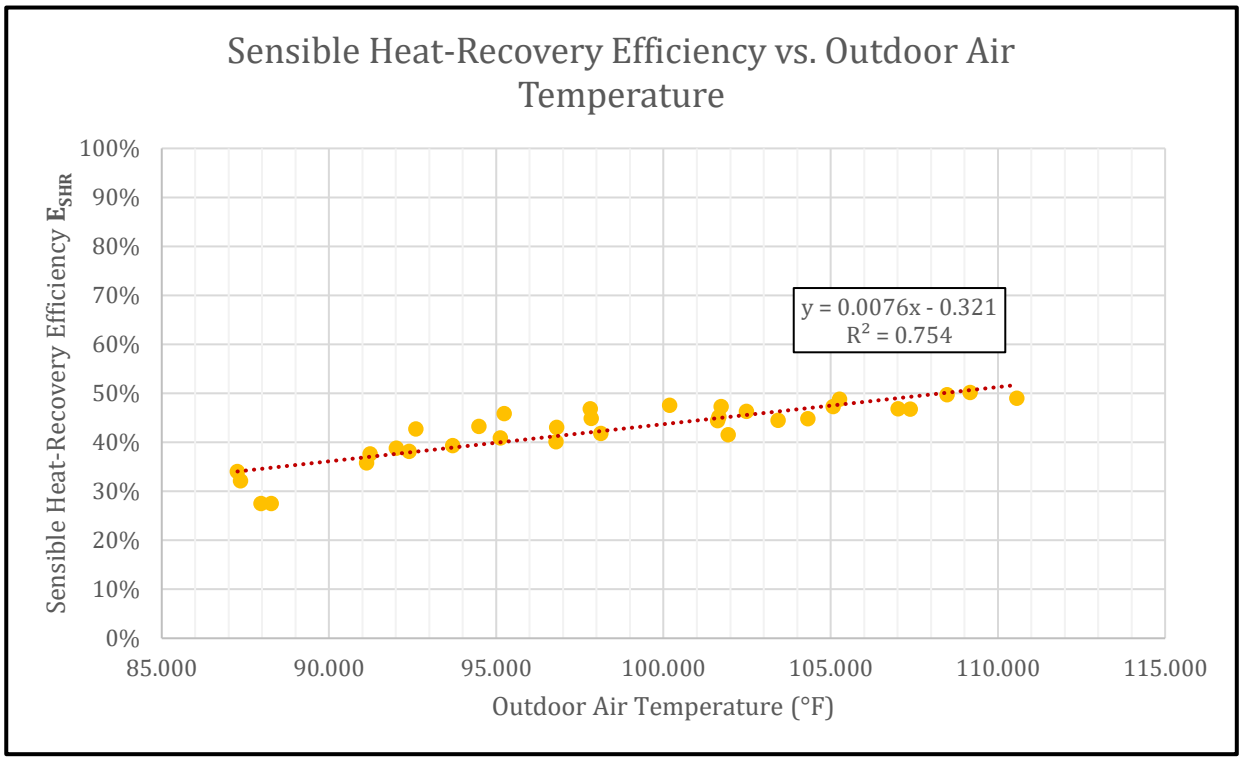

Figure 23. Linear Trendline Applied to E_{SHR} vs. Outdoor Air Temperature

As shown in Figure 23, the coefficient representing the slope of the linear trendline is 0.0076 and the constant representing the intercept is -0.321. The R-squared value is 0.754. Although low in magnitude, the positive nature of the coefficient in the trendline equation indicates

a positive correlation between sensible heat-recovery efficiency E_{SHR} and outdoor air temperature. The R-squared value is 0.754, which indicates that the linear model explains most of the variability of the response data (i.e. E_{SHR}) around its mean. Compared to the R-squared value from Figure 21, which was 0.854, the R-squared value of 0.754 for the linear trendline applied in Figure 23 is lower. Similar to the plot of apparent effectiveness ε, the comparison between the R-squared values from Figure 21 and Figure 23 is to be expected due to the increased scatter in data. In Figure 21, the E_{SHR} was averaged for all of the tests conducted at each heater set point. In Figure 23, the E_{SHR} of each individual test is plotted against the recorded outdoor air temperature of each individual test. As such, the R-squared value of the linear trendline applied to the individual test data points is lower compared to the averaged test data points. Despite the lower R-squared value, however, a coefficient of determination of 0.754 points towards the linear model fitting the data reasonably well.

To continue the investigation, a determination of the statistical significance of the association between the response variable (E_{SHR}) and the term (outdoor air temperature) was made. Such a determination was made by comparing the p-value of the term (outdoor air temperature) to a significance level of 0.05 to assess the null hypothesis. In the case of this study, the null hypothesis is that the association between E_{SHR} and outdoor air temperature is not statistically significant. Should the p-value of the linear regression be less than or equal to 0.05 (the significance level α), then the null hypothesis is rejected. After applying the linear regression shown in Figure 23 and utilizing the Data Analysis package in Microsoft Excel, it was found that the p-value for the term (outdoor air temperature) is approximately 5.86E-11, which is near zero. Hence, with p-value < α, we reject the notion that the association is not statistically significant.

Therefore, there is a statistically significant association between sensible heat-recovery efficiency E_{SHR} and outdoor air temperature.

In order to substantiate the linear regression model applied, two additional assumptions were verified. The first assumption that was verified was that the residuals are randomly distributed. The following Figure 24 illustrates the residuals versus fits plot for the apparent effectiveness linear regression model.

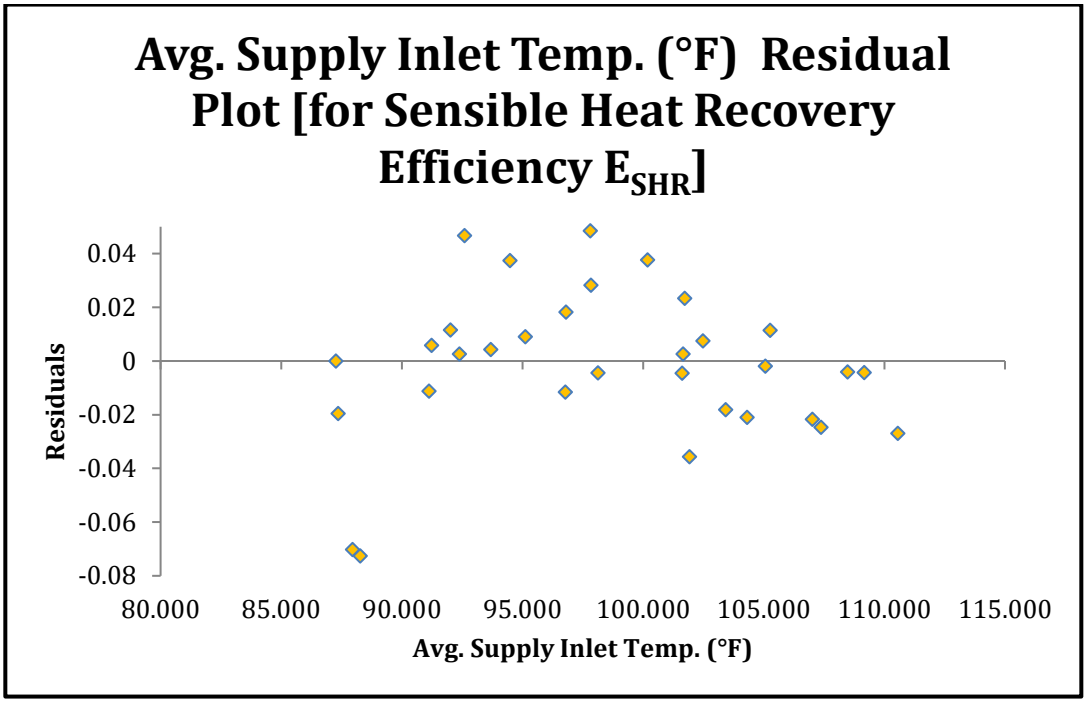

Figure 24. Residuals vs. fits plot for Sensible Heat-Recovery Efficiency

As depicted in Figure 24, the points appear randomly scattered on the plot, which is ideal. It is worth noting that there are two outliers towards the bottom of the plot. The two outliers have residual values of approximately -0.08, indicating that the E_{SHR} from these two data points are lower than the fitted value offered by the linear regression. Despite the presence of these two outliers, the overall residuals versus fits plot has no identifiable pattern that is visible. Therefore, given the current data set, the first assumption of random distribution of residuals is verified.

Conducting additional tests on the HRV for E_{SHR} within the studied outdoor air temperature range is advisable for a strengthened verification.

The second assumption that was verified was that the residuals are normally distributed. The following Figure 25 illustrates the normal probability plot for the E_{SHR} linear regression model.

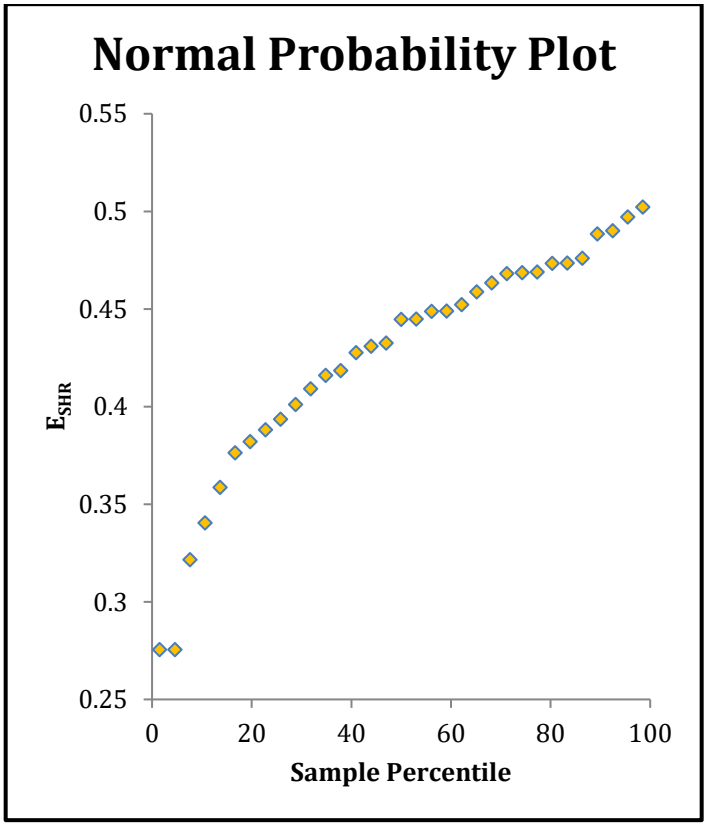

Figure 25. Normal probability plot for Sensible Heat-Recovery Efficiency

As seen in Figure 25, a majority of the residuals generally appear to follow a straight line. However, there are two outliers, namely, the two residuals with E_{SHR} values closer to 0.275, or 27.5%. The two outliers are the same as those identified in the plot of residuals versus fits in Figure 24. Assuming that the two outliers were potentially the result of inconsistent regulation of the duct heater temperature, then a reexamination of the normal probability plot can be made. The following

Figure 26 illustrates the normal probability plot that was featured in Figure 25 minus the two outlier residuals.

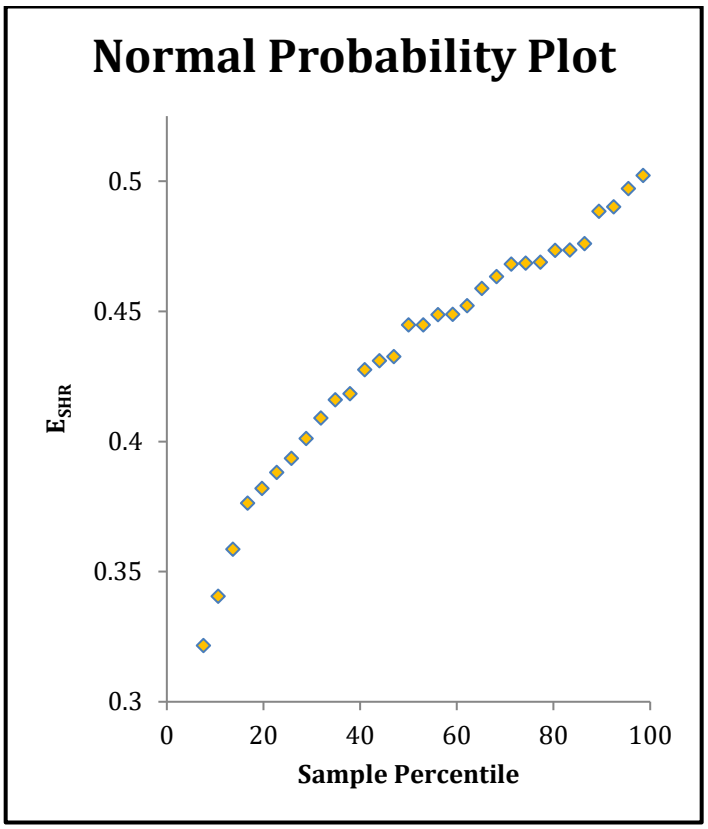

Figure 26. Outliers removed from E_{SHR} normal probability plot

As depicted in Figure 26, the normal probability plot features residuals that appear to follow a straight line. With the outliers aside, it is assumed that the residuals are normally distributed in regards to the linear regression for sensible heat-recovery efficiency. Said outliers could be the result of inconsistencies during the data collection period of 10 minutes during testing. The inconsistencies could be sourced to uneven regulation of power to the duct heater or some deviations in performance for the fans in the duct system. Ideally for future analysis, more tests would be conducted to produce a larger dataset.

6. FUTURE STUDIES

The foundations of studying the thermal and airflow performance of heat recovery ventilators (HRVs) have been established. Currently, data on the velocity, temperature, static pressure, CO_2 content, and relative humidity of the air moving through recovery ventilation systems can be measured, recorded, and analyzed. In addition, the current setup allows for flexibility in mounting methods of HRVs as well as the heating of incoming supply air to the ventilation system.

One area of future improvement involves studying supply air that is cooled to a lower temperature. Currently, the performance studies have involved the heating of incoming air to simulate warmer outdoor conditions such as those found during the summertime. An expansion to the performance study could involve the simulation of colder outdoor environment conditions such as those found during the wintertime. Such a simulation could be achieved by installing a cooling coil into the duct network at the supply inlet. Furthermore, to add an additional element of control to the system, a heater or cooler could also be installed at the exhaust inlet region. The presence of a heater or cooler at both the supply inlet and the exhaust inlet offers increased options for the combination of air temperatures that enter the ventilation system.

A second area of future improvement involves the introduction of moisture to the supply inlet air that is fed into the ventilation system. Such an area of improvement would be intended for the future study of energy recovery ventilators, or ERVs, that transfer both moisture and heat between the two moving airstreams. Moisture can be introduced to the supply inlet air by means of a steam humidifier that has a steam hose integrated into the supply inlet duct. The steam humidifier addition to the test setup adds another degree of variability to the air conditions flowing through the ventilation system but would be essential to characterizing ERV performance.

Furthermore, the variation of humidity that is introduced to the system can be studied independently of or simultaneously with the heating or cooling of incoming supply inlet air to the ventilation system. Overall, the addition of moisture to the duct system by means of a steam humidifier expands the testing capability and future certification of recovery ventilation systems.

7. CONCLUSIONS

Heat recovery ventilators, or HRVs, are devices that help maintain comfort within residential spaces. HRVs exhaust stale indoor air and supply fresh outdoor air while also transferring heat between the two airstreams via a heat exchange core. Useful during times of the year when outdoor temperatures are at their extremes, HRVs provide a means of contributing towards residential ventilation and reclamation of heat that would otherwise be rejected outdoors. Given the energy benefits of HRVs in terms of efficiency and savings, a thesis project focusing on the thermal operations of these devices was inspired. In particular, this thesis project centers on: (1) designing and constructing a test setup for data collection on HRVs, (2) acquiring a large data base of HRV test data for a wide range of outdoor air temperatures, and (3) using the data base to determine the parameters of apparent effectiveness, ε, and sensible heat-recovery efficiency, E_{SHR}, of an HRV.

An important task in this research was the design and construction of a test rig for the mounting and testing of recovery ventilators and for the collection of a data base to characterize device effectiveness and efficiency. An important parameter and variable during testing and analysis was the supply inlet airstream temperature that was achieved and varied by using an electric duct heater. Using the above test rig, a total of 33 tests were conducted on the Fantech SHR200 HRV at a rated volumetric flow rate of 195 CFM and outdoor air temperatures ranging from 88 °F to 112 °F, with five specific test values being 90 °F, 95 °F, 100 °F, 105 °F, and 110 °F. Of special importance, two parameters known as apparent effectiveness, ε, and sensible heat-recovery efficiency, E_{SHR}, which are of interest for characterizing HRV performance, are analyzed using the contents of the data base.

Directly proportional relationships were identified for both ε and E_{SHR} versus outdoor air temperature. As the hot outdoor air temperature increased from about 88 °F to 112 °F, the value of ε increased from a low of 55% to a high of 60%. For ε versus outdoor air temperature, the R-squared value of the linear regression was 0.3155, indicating that some of the linear model fits the data. Furthermore, for the same hot outdoor air temperature increase as noted above, E_{SHR} increased from a low of 32% to a high of 48%. For E_{SHR} versus outdoor air temperature, the R-squared value of the linear regression was 0.7540, indicating that most of the linear model fits the data. To summarize, sensible heat-recovery efficiency versus outdoor air temperature is better fitted by a linear model as compared to apparent effectiveness versus outdoor air temperature within the studied temperature range. The application of linear regression was verified by plotting residuals versus fits and normal probability plots for the data sets associated with ε and E_{SHR}. In addition, the statistical significance between ε and outdoor air temperature and between E_{SHR} and outdoor air temperature was supported by the results of a p-test. From the p-test, the p-value of the ε data set was 0.00067 and the p-value of the E_{SHR} data set was 5.86E-11. With both p-values being less than a significance value of 0.05, one can deem that statistically significant relationships exist between ε and outdoor air temperature and between E_{SHR} and outdoor air temperature. The above statistical methods support the investigation of how outdoor air temperature affects HRV performance within the studied temperature range, which is presented in the next paragraph.

Apparent effectiveness, ε, and sensible heat-recovery efficiency, E_{SHR}, were found to be linearly proportional to hot outdoor air temperatures over a range of approximately 88 °F to 112 °F, with actual set points during testing being 90 °F, 95 °F, 100 °F, 105 °F, and 110 °F. Of specific importance, both ε and E_{SHR} increase as hot outdoor air temperature increases from minimum to maximum, with ε increasing modestly by approximately 5% and E_{SHR} increasing appreciably by

approximately 16%. From the results, one can conclude that HRV performance does not diminish as hot outdoor air temperature increases. Instead, HRV performance seemingly adapts to the increase in hot outdoor air temperature and responds with an increase in apparent effectiveness and sensible heat-recovery efficiency. The increase in E_{SHR} is more pronounced than the increase in ε within the studied temperature range, but nevertheless both parameters increase, meaning an improved performance results from temperature increases. Such a conclusion can assure engineers that HRVs are reliable performers while in cooling mode characteristic of hot outdoor air temperatures, which should promote the use and selection of HRVs for HVAC system design.

Understanding the performance of heat recovery ventilators in a controlled environment, as was performed in this research, provides meaningful insights for HRV manufacturers, while additional refined performance studies in the same lab setting can also provide third-party feedback on a product's rated airflow and thermal performance. Of special importance, this third-party feedback via a performance study leads to HRV certifications prior to product distribution to the consumer market. In essence, a refined performance study helps ensure that the manufacturer releases a product that genuinely performs as advertised.

REFERENCES

[1] Klenck, Thomas. “How It Works: Heat Recovery Ventilator.” *Popular Mechanics*, Popular Mechanics, 14 Nov. 2017, www.popularmechanics.com/home/interior-projects/how-to/a149/1275121/.

[2] Canada Standards Association. *Standard laboratory methods of test for rating the performance of heat/energy-recovery ventilators.* C439-09.

[3] Air Movement and Control Association International. *Laboratory Methods of Testing Fans for Certified Aerodynamic Performance Rating.* ANSI/AMCA Standard 210-16 / ASHRAE Standard 51-16.

[4] Editor, Minitab Blog. “Regression Analysis: How Do I Interpret R-Squared and Assess the Goodness-of-Fit?” *Minitab Blog*, 2013, blog.minitab.com/blog/adventures-in-statistics-2/regression-analysis-how-do-i-interpret-r-squared-and-assess-the-goodness-of-fit.

[5] Support, Minitab. “Interpret the Key Results for Fitted Line Plot.” 2019, support.minitab.com/en-us/minitab/18/help-and-how-to/modeling-statistics/regression/how-to/fitted-line-plot/interpret-the-results/key-results/.

[6] LaMorte, Wayne W. “Central Limit Theorem.” *The Role of Probability*, Boston University School of Public Health, 2016, sphweb.bumc.bu.edu/otlt/mph-modules/bs/bs704_probability/BS704_Probability12.html.

APPENDIX

Table 3. Test setup sensors and their measurement ranges and accuracies

Sensor Name	Sensor Category	Operating Range	Measurement Accuracy
Dwyer CDTR-2D4D4 (Duct Version)	CO2/RH/Temp Transmitter	CO2: 0 to 2000 PPM	CO2: ± 40 PPM ± 3% of reading
		Temperature: 32 to 122 °F (0 to 50 °C)	Temperature: ± 1 °C @ 25 °C
		RH: 0 to 100%	RH: ± 2%
E+E Elektronik EE650	Air Velocity Transmitter	0 to 20 m/s (0 to 4000 ft/min)	At 20 °C (68 °F), 45% RH, 1013 hPa:
			0.2...20 m/s (40...4000 ft/min)
			± (0.2 m/s (40 ft/min) + 3% of m. v.)
OMEGA Type T Thermocouple	Thermocouple	-250 °C to 350 °C (-418 °F to 662 °F)	Standard Limits of Error: Greater of
			2.2 °C or 0.75%
			Special Limits of Error: Greater of
			1.1 °C or 0.4%
Setra Model 264	Differential Pressure Transducer	Variable	± 1.0% Full Scale (standard)
		Compensated range °F (°C)	0.10% FS (Hysteresis)
		0 to +150 (-18 to +65)	
		Zero shift %FS/100°F(50°C)	
		± 0.033 (±0.06)	
		Span shift %FS/100°F(50°C)	
		± 0.033 (±0.06)	